Received: 27 October 2020 | Revised: 20 January 2021 | Accepted: 21 January 2021

DOI: 10.1002/jccs.202000475

ARTICLE

JOURNAL OF THE CHINESE CHEMICAL SOCIETY

Synthesis of hydantoin alkynes through palladium-catalyzed reaction, antibacterial evaluation, and molecular docking studies

Ali Keivanloo[1] | **Saeed Lashkari**[1] | **Saghi Sepehri**[2] | **Mohammad Bakherad**[1] | **Sima Abbaspour**[1]

[1]Faculty of Chemistry, Shahrood University of Technology, Shahrood, Iran

[2]Department of Medicinal Chemistry, School of Pharmacy, Ardabil University of Medical Sciences, Ardabil, Iran

Correspondence
Ali Keivanloo, Faculty of Chemistry, Shahrood University of Technology, Shahrood 36199-95161, Iran.
Email: akeivanloo@yahoo.com

Saghi Sepehri, Department of Medicinal Chemistry, School of Pharmacy, Ardabil University of Medical Sciences, Ardabil, Iran.
Email: sepehri.saghi@yahoo.com

Funding information
the Research Council

Abstract

Novel 3-(3-(aryl)prop-2-yn-1-yl)-5,5-diphenylimi- dazolidine-2,4-diones were synthesized through the reaction of 5,5-diphenyl-3-(prop-2-yn-1-yl)imidazolidine-2,4-dione and aryl iodides in the presence of a palladium-copper catalytic in CH_3CN at room temperature. All prepared compounds were examined against the two bacterial strains, *Micrococcus luteus* and *Pseudomonas aeruginosa* and subjected by molecular docking studies. The in silico study carried out to predict the conformation of the examined compounds recommended that these compounds could bind noticeably to key the residues at the active site of dihydropteroate synthase. The interactive, biochemical, and in silico studies were in concordance with each other.

KEYWORDS

antibacterial activity, aryl iodide, imidazolidine-2,4-dione, molecular docking, palladium catalyst

1 | INTRODUCTION

The palladium-catalyzed reaction of terminal acetylenic compounds with aryl and vinyl halides catalyzed by copper(I) salt in the presence of amine base has been known as Sonogashira coupling. The Sonogashira coupling is one of the most important and powerful approaches for C—C bond-forming and construction of aryl alkynes.[1,2] Aryl alkynes are valuable intermediates in organic synthesis and are applied for the preparation of natural products,[3] biologically active compounds,[4] molecular electronics,[5] and polymers.[6]

Imidazoledin-2,4-diones (hydantoins) have been known compounds for more than a century since their discovery.[7] Hydantoins are important nitrogen heterocyclic compounds in organic synthesis and pharmaceutical chemistry. Diverse procedures have been extended for the synthesis of hydantoins,[8] which have essentially created a hydantoin nucleus with substituents at various positions. Thus, the synthesis of hydantoins is an extremely active area of investigation,[9] and it is necessary to develop effective methods for construction of a variety of hydantoin derivatives with substituents at the favorite positions. It is well-known that hydantoins are important biologically active compounds display properties, including anti-ulcer,[10] antitumor,[11] antiviral,[12] antibacterial,[13] antidiabetic,[14] antiarrhythmic,[15] and anticonvulsant[16] activities. They also have herbicidal and antifungal properties and are used for agrochemical applications.[17] For example, hydantoins **A1**, **A2**, and **A3** used as anticonvulsant,[18] fungicidal,[16,19] and antibacterial agents, [20] respectively (Figure 1).

Previously we reported the synthesis of new biologically active compounds via Sonogashira reactions,[21,22] in this research, we present the synthesis of novel 3-(3-(aryl)prop-2-yn-1-yl)-5,5-diphenylimidazolidine-2,4-dione derivatives through Sonogashira coupling reaction. The newly

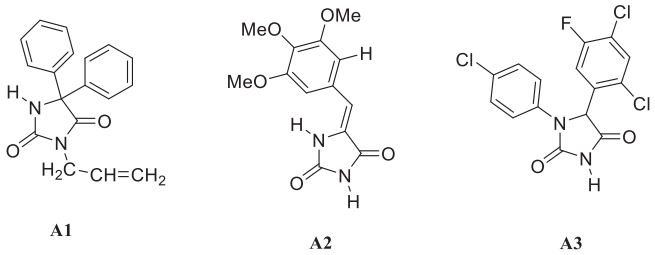

FIGURE 1 Examples of biologically active molecules containing a hydantoin core

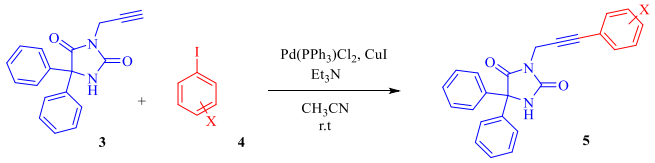

SCHEME 1 Synthesis of 3-(3-(aryl)prop-2-yn-1-yl)-5,5-diphenylimidazolidine-2,4-dione (**5**) from the reaction of 5,5-diphenyl-3-(prop-2-yn-1-yl)imidazolidine-2,4-dione (**3**) and an Aryl iodide (**4**)

synthesized compounds were examined for their antibacterial activities and were exposed to the molecular docking studies.

2 | RESULTS AND DISCUSSION

In this study, we describe the preparation of novel 3-(3-(aryl) prop-2-yn-1-yl)-5,5-diphenylimidazolidine-2,4-dione derivatives **5** by coupling reaction of 5,5-diphenyl-3-(prop-2-yn-1-yl)imidazolidine-2,4-dione **3** with aryl iodides **4** catalyzed by $Pd(Ph_3P)_2Cl_2$ and CuI in CH_3CN at room temperature (Scheme 1).

The reaction of benzil and urea in alkaline EtOH afforded 5,5-diphenylimidazolidine-2,4-dione (**1**) as starting material.[23] the reaction of compound 1 with propargyl bromide (**2**) in the presence of K_2CO_3 in DMF as solvent yielded 5,5-diphenyl-3-(prop-2-yn-1-yl) imidazolidine-2,4-dione 3 in high yield (Scheme 2).

For optimization of the reaction conditions, we selected the reaction of 5,5-diphenyl-3-(prop-2-yn-1-yl) imidazolidine-2,4-dione (**3**) and 1-iodo-4-nitrobenzene 4c as a model system. First, we carried out the reaction of 5,5-diphenyl-3-(prop-2-yn-1-yl)imidazolidine-2,4-dione (1.0 mmol) with 1-iodo-4-nitrobenzene (1.2 mmol) in the presence of $Pd(Ph_3P)_2Cl_2$/CuI and Et_3N, in CH_3CN at room temperature. Under this condition, the desired product, 3-(3-(4-nitrophenyl)prop-2-yn-1-yl)-5,5-diphenyl imidazolidine-2,4-dione **5c**, was prepared in a 96% yield (Table 1, entry 4). The effects of solvents, bases, catalysts, and temperatures on the reaction were further examined.

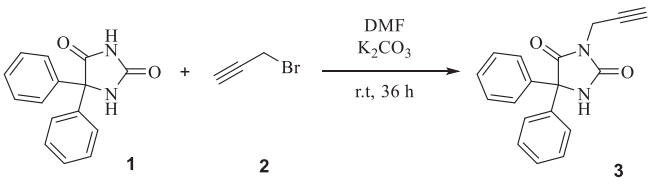

SCHEME 2 Synthesis of 5,5-diphenyl-3-(prop-2-yn-1-yl) imidazolidine-2,4-dione (**3**) from the reaction of 5,5-diphenylimidazolidine-2,4-dione (**1**) with 3-bromoprop-1-yne (**2**) in the presence of K_2CO_3

The results are outlined in Table 1. The solvents, including CH_3CN, DMSO, THF, and DMF, and the organic and inorganic bases, including K_2CO_3, Cs_2CO_3, Et_3N, and morpholine were investigated. It was realized that CH_3CN was the best solvent and Et_3N was the most effective and suitable base for the coupling reaction. Moreover, we studied several palladium catalysts, including $Pd(OAc)_2$, $Pd(PPh_3)_2Cl_2$, and Pd/C in the presence and absence of a copper co-catalyst. $Pd(PPh_3)_2Cl_2$ was found to be the efficient catalytic system and gave the target product with a high reaction yield. Besides, the use of CuI was found to be necessary for reaction progress. When the base Et_3N was replaced by K_2CO_3 or the solvent CH_3CN was replaced by DMSO, the reaction yields decreased to 69 and 65%, respectively (Table 1, entries 1 and 7). As shown in Table 1, the desired product **5c** was produced in a 70% yield when the reaction was accomplished in the presence of Et_3N and $Pd(PPh_3)_2Cl_2$/CuI in DMF at r.t. (entry 5). In addition, the desired product **5c** was formed in a 60% yield when the reaction was done in the presence of Cs_2CO_3 and $Pd(OAc)_2$/CuI in DMF at r.t. (entry 10). Besides, the convenient reaction temperature was room temperature.

With the results of our optimization reaction in hand, we then investigated the scope and generality of the reaction, by the reaction of 5,5-diphenyl-3-(prop-2-yn-1-yl) imidazolidine-2,4-dione (**3**), with aryl iodides **4a–g** in the presence of $Pd(PPh_3)_2Cl_2$ at room temperature to afford 3-(3-(aryl)prop-2-yn-1-yl)-5,5-diphenylimidazolidine-2,4-diones **5a–g**. The results are shown in Table 2.

The structure of new compounds **5a–g** was characterized by spectroscopic data, mass, and elemental analysis. For example, in the ^{1}H-NMR spectrum for **5c**, the NH proton of imidazole ring appeared as a singlet at δ(H) 9.79, which disappeared upon deuteration. Two doublets were observed at δ(H) 8.18 and 7.65 characteristics of the aryl group. Two phenyl groups appeared as a multiplet at δ(H) 7.37–7.47 with 10 protons area. In the aliphatic region, the methylene group protons appeared as a singlet at δ(H) 4.31. In addition, the ^{13}C NMR spectrum of **4a** presented 14 peaks, accounting for all carbon atoms. Molecular ion peak at m/z 411 was recorded by

TABLE 1 Effects of solvent, catalysts, base, and temperature on the reaction of 5,5-diphenyl-3-(prop-2-yn-1-yl)imidazolidine-2,4-dione and 1-iodo-4-nitrobenzene afford 3-(3-(4-nitrophenyl)prop-2-yn-1-yl)-5,5-diphenylimidazolidine-2,4-dione[a]

Entry	Catalyst	Solvent	Base	T/°C	Yield (%)
1	$Pd(PPh_3)_2Cl_2$/CuI	CH_3CN	K_2CO_3	r.t	69
2	$Pd(PPh_3)_2Cl_2$/CuI	CH_3CN	Morpholine	r.t	75
3	$Pd(PPh_3)_2Cl_2$/CuI	CH_3CN	Cs_2CO_3	r.t	81
4	$Pd(PPh_3)_2Cl_2$/CuI	CH_3CN	Et_3N	r.t	96
5	$Pd(PPh_3)_2Cl_2$/CuI	DMF	Et_3N	r.t	70
6	$Pd(PPh_3)_2Cl_2$/CuI	DMF	Morpholine	50	71
7	$Pd(PPh_3)_2Cl_2$/CuI	DMSO	Et_3N	r.t	65
8	$Pd(PPh_3)_2Cl_2$/CuI	DMSO	K_2CO_3	50	72
9	$Pd(OAc)_2$/CuI	DMF	K_2CO_3	50	68
10	$Pd(OAc)_2$/CuI	DMF	Cs_2CO_3	r.t	60
11	$Pd(OAc)_2$/CuI	DMSO	Cs_2CO_3	50	64
12	$Pd(OAc)_2$/CuI	DMSO	Et_3N	r.t	72
13	$Pd(OAc)_2$/CuI	CH_3CN	Cs_2CO_3	50	65
14	$Pd(OAc)_2$/CuI	CH_3CN	K_2CO_3	r.t	61
15	$Pd(PPh_3)_2Cl_2$	CH_3CN	Morpholine	40	54
16	$Pd(PPh_3)_2Cl_2$	DMF	Et_3N	r.t	50
17	$Pd(PPh_3)_2Cl_2$	THF	K_2CO_3	r.t	47
18	$Pd(PPh_3)_2Cl_2$	DMSO	Cs_2CO_3	40	51
19	Pd/C, CuI	CH_3CN	Morpholine	50	46
20	Pd/C, CuI	DMF	K_2CO_3	40	41

[a]Reaction conditions: A mixture of **3** (1.2 mmol), **4** (1.0 mmol), $Pd(PPh_3)_2Cl_2$ (0.05 mmol), CuI (0.1 mmol), and base (10 mmol) in solvent (4 ml) stirred for 10 hr.

the mass spectrometer. The FT-IR and microanalysis data were consistent with the proposed structure.

Mechanistically, Sonogashira coupling reaction comprises a general multi-step process as shown in Scheme 3. First, the Pd(0) was formed by the in situ reductions of Pd(II) in the reaction mixture. In continuing, oxidative addition of aryl iodide by Pd(0) produces complex intermediate A, followed by trans-metalation from copper acetylide (B), trans-cis isomerization (C), and reduction-elimination (D) afford final product 5.

2.1 | Antibacterial assay

All newly synthesized 3-(3-(aryl)prop-2-yn-1-yl)-5,-5-diphenylimidazolidine-2,4-diones **5a–g** were examined for in vitro antibacterial activities against tow bacterial strains, *Micrococcus luteus* and *Pseudomonas aeruginosa* by the well diffusion method. DMSO was selected as the negative control, displaying without activity against the bacterial strains examined, and tetracycline was selected as a positive control. The obtained results are shown in Table 3. The evaluation was performed at a concentration of 1,000 μg/ml in DMSO and the results were reported as the inhibition zone in mm. All compounds showed antibacterial activities against *M. luteus* and *P. aeruginosa*. The structure–activity relationship in compounds **5a–g** showed that **5d** and **5f** have better inhibitory activity than the others against *M. luteus* and *P. aeruginosa*. In addition, **5b**, **5d**, **5e**, and **5f** has better inhibitory activity than the others against *M. luteus*, **5d** and **5f** have better inhibitory activity against *P. aeruginosa*.

2.2 | The molecular docking simulation studies

A crucial stage in the biosynthesis of dihydropteroate and pyrophosphate is the condensation of 6-hydroxymethyl-7,-8-dihydropterin pyrophosphate with *para*-aminobenzoic acid (*p*ABA) that is catalyzed by the enzyme dihydropteroate synthase (DHP), which is a significant biosynthetic process for micro-organisms. In the biosynthesis of pyrimidines, purines, and certain amino acids in living cells, folate derivatives are critical cofactors.[24]

TABLE 2 Synthesis of 3-(3-(aryl)prop-2-yn-1-yl)-5,5-diphenylimidazolidine-2,4-diones (**5**)[a]

Entry	Aryl iodide	Product	Melting point (°C)	Yield (%)
1	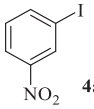 **4a**	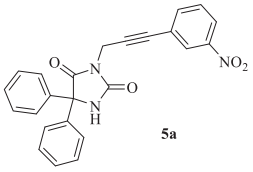 **5a**	105–106	90
2	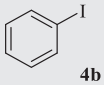 **4b**	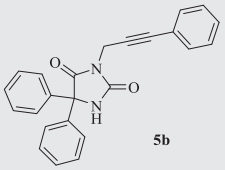 **5b**	102–103	87
3	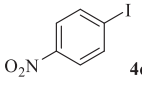 **4c**	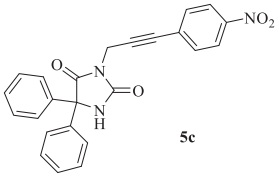 **5c**	110–111	96
4	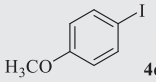 **4d**	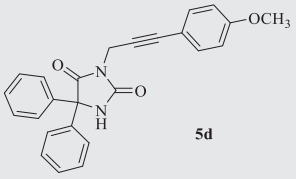 **5d**	98–100	82
5	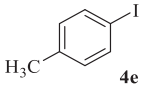 **4e**	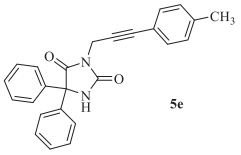 **5e**	106–107	80
6	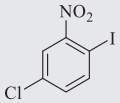 **4f**	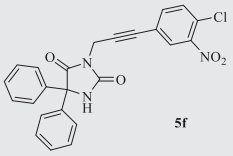 **5f**	115–118	83
7	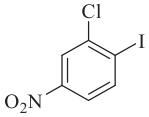 **4g**	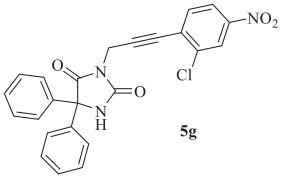 **5g**	120–121	81

[a]Reaction conditions: A mixture of **5** (1.0 mmol), **6** (1.2 mmol), $Pd(PPh_3)_2Cl_2$ (0.05 mmol), CuI (0.1 mmol), and base (10 mmol) in solvent (4 ml) stirred at r.t for 12 hr.

Thus, significant goals for the design and development of new antibacterial drugs, are most of the enzymes in the folate biosynthesis pathway. The first efficient synthetic antimicrobial drugs that are still extensively used in clinical, are sulphonamide drugs. These drugs group as analogs of *p*ABA for DHP enzyme inhibit folate biosynthesis and can so efficiently diminish the cell of folate cofactors.[25] The synthesized compounds in this research have structural similarity with sulphonamide drugs, for example, sulfamethoxazole (Figure 2).

2.3 | Validation of molecular docking

The presentation of a public docking technique can be verified through testing its validation to predict the most essential affinity of a cognate (co-crystallographic) ligand.[26] This technique was the presentation using eliminating the cognate ligand and re-docking it into its protein (self-docking). The rule of the docking validation is Root-mean-square deviation (RMSD) of the Cartesian coordinates of the atoms of the compound in the docked

and crystallographic conformations (RMSD < 2 Å). In this research, sulfamethoxazole (co-crystallographic) ligand of DHP was re-docked into protein and RMSD value of validation of molecular docking for protein with Protein Data Bank (PDB) ID: 3TYE obtained 0.49 Å. The descriptions of sulfamethoxazole interaction with the DHP active site showed six hydrogen bonds including: Two hydrogen bonds between NH_2 group at para phenyl ring of sulfamethoxazole and carboxyl of ASP184 and carbonyl group of ASN120 residues, two hydrogen bonds between oxygen atom of SO_2 of ligand and amine groups of ARG254 residue, a hydrogen bond between NH of ligand and carboxyl group of ASP110 residue and a hydrogen bond between NH at oxazole ring of sulfamethoxazole and hydroxyl group of THR67 residue. In addition, MET145, ILE122, PHE189, and GLY64 residues exhibited hydrophobic interactions with ligand. Suitable interactions and strong binding with main amino acid residues at the active site of DHP is designated by the free binding energy values ($\Delta G_{binding}$), expressed in term kcal/mol.

2.4 | Binding mode of studied compounds

Molecular docking results exhibited that screened compounds **5a–g** could inhibit DHP by hydrophobic and hydrogen bond interactions (Tables 4 and 5).

Among the docked compounds, compounds **5e** having a methyl group at the *para* position of the phenyl rings revealed the best docking score and the highest antibacterial activity (Tables 3–5). The binding mode of compound **5e** into DHP active site was revealed in Figure 3. The hydantoin moiety of **5e** situated at the hydrophobic pocket, enclosed using the amino acids GLU65, ASP101, ASP61, GLY63, GLY64, ASN27, ILE25, LEU26, and ILE62 making a strong hydrophobic binding. Comprehensive investigation indicated that the phenyl group of **5e** made two cation-π stacking interactions through the amino acids ARG254 and LYS220. It was

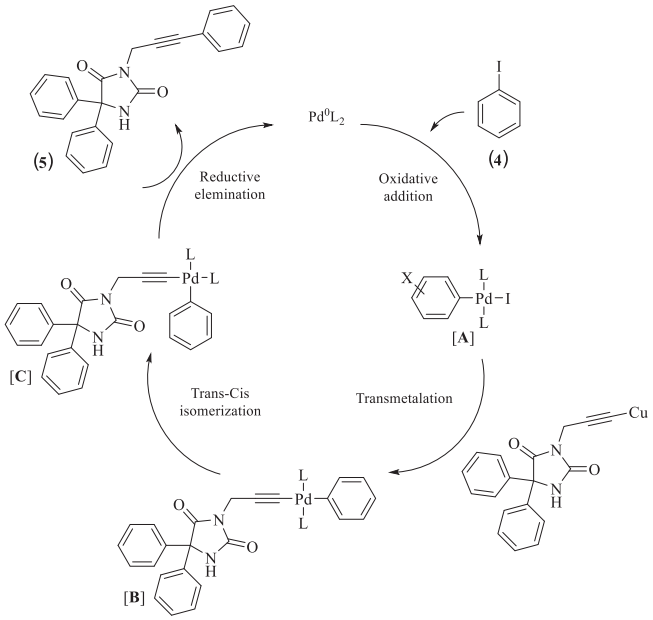

SCHEME 3 Proposed mechanism for formation of 3-(3-(aryl) prop-2-yn-1-yl)-5,5-diphenylimidazolidine-2,4-diones from the reaction of 5,5-diphenyl-3-(prop-2-yn-1-yl)imidazolidine-2,4-dione and aryl iodides

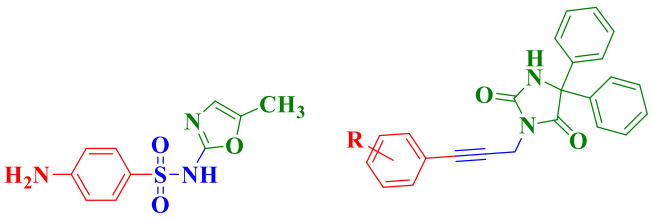

Sulfamethoxazole **Compounds 5a-g**

FIGURE 2 Synthesized compounds (**5a–g**) with structural similar to sulfamethoxazole

TABLE 3 Antibacterial activities of selected compounds (1,000 μg/ml) as inhibition zone in mm

Entry	Compound	*Micrococcus luteus*	*Pseudomonas aeruginosa*
1	**5a**	8	6
2	**5b**	41	12
3	**5c**	24	9
4	**5d**	41	16
5	**5e**	42	10
6	**5f**	41	14
7	**5g**	31	9
8	DMSO	—	—
9	Tetracycline	41	13

TABLE 4 Docking results of **5a–g** derivatives docked into DHP target

Compound	Hydrogen bond	Hydrophobic interaction	π-π	Cation-π
5a	NH_2 of ARG254 with O of NO_2	SER218, HIS256, GLY188, THR67, LYS220, ASP101, PHE189, ILE122, ASN120, MET145, GLY216, ASP184	—	ARG254 with ph
5b	NH_2 of ARG254 with O of C═O	ILE25, LEU26, GLY63, ASN27, ILE62, ASP61, GLU65, GLY64, ASP101, SER66, PHE189, ASN120, THR67, ILE122, MET145	—	ARG254 with ph LYS220 with ph
5c	NH_2 of ARG254 with O of NO_2 NH of SER221 with O of C═O	PHE222, GLY188, ASN196, ARG234, PHE189, LYS220, ARG219, SER218, HIS256, ILE25	HIS256 with ph PHE189 with ph	—
5d	NH_2 of ARG254 with O of C═O	LEU26, ILE25, GLY63, ILE62, ASN27, GLU65, THR67, ASP61, SER66, GLY64, PHE189, ASP101, MET145, ASN120, ILE122, ILE143, ASP184	—	—
5e	NH_2 of ARG254 with O of C═O	ILE25, ASN27, LEU26, ILE62, GLY64, GLU65, GLY63, ASP61, ASP101, SER66, THR67, ILE122, PHE189, ASN120, MET145, ASP184	—	ARG254 with ph LYS220 with ph
5f	NH_2 of ARG254 with O of NO_2	ASN196, SER221, PHE222, GLY188, LYS220, PHE189, GLY216, ASP101, ILE122	—	—
5g	NH_2 of ARG254 with O of NO_2 NH_2 of LYS220 with O of NO_2	GLY188, ASN196, PHE222, PHE189, SER218, LYS220, ARG219, HIS256	PHE189 with ph	—

TABLE 5 Docking results of lead compounds docked into theDHP

Compound	ΔG_{bind} (kcal/mol)	VHDE[a] (kcal/mol)	EE[b] (kcal/mol)	IE[c] (kcal/ol)
5a	−6.95	−7.64	−0.80	−8.44
5b	−7.69	−8.52	−1.26	−9.78
5c	−7.13	−7.89	−1.03	−8.92
5d	−7.92	−8.34	−1.67	−10.01
5e	−8.13	−8.95	−1.27	−10.22
5f	−7.52	−8.58	−1.04	−9.61
5g	−7.35	−7.90	−0.94	−8.84

[a]VanderWaals-Hbond-Desolvation-Energy.
[b]Electrostatic Energy.
[c]Intermolecular Energy.

exposed that the residue ARG254 (bond length: 1.90 Å) made a hydrogen bond with **5e**, which was the main interaction of **5e** with DHP. All these interactions aided **5e** to stability in the DHP active site.

According to docking results, compounds **5d** and **5e** exposed the lowest free binding energy among compounds. These compounds are having methoxy and methyl groups at the *para* position of the phenyl ring, respectively. Compound **5d** indicated weaker antibacterial activity and free binding energy than **5e**. It seems that the existence of hydrophilic group at the *para* position of phenyl ring declines antibacterial activity and free binding energy due to the reduction of lipophilicity. In addition, compound **5e** exhibited two cation-π stacking interactions with LYS220 and ARG254 residues while compound **5d** did not show any cation-π stacking interaction. LYS220 residue in loop 2 of DHP has an important role to stabilize the binding of *p*ABA at the active site.[27]

Compound **5b** showed antibacterial activity and free binding energy as well as **5d**. Compound **5b** is without group on *para* position of the phenyl ring and decreases lipophilicity in compared to **5d** and **5e**. On the other hand, compound **5b** formed two cation-π stacking inter-

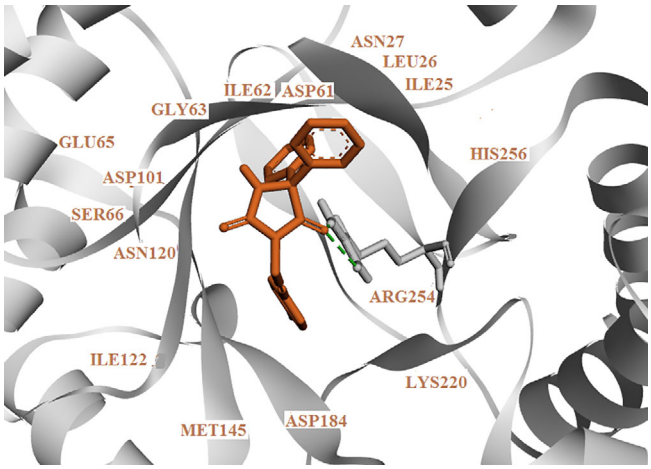

FIGURE 3 Binding mode of compound **5e** in the dihydropteroate synthase active site

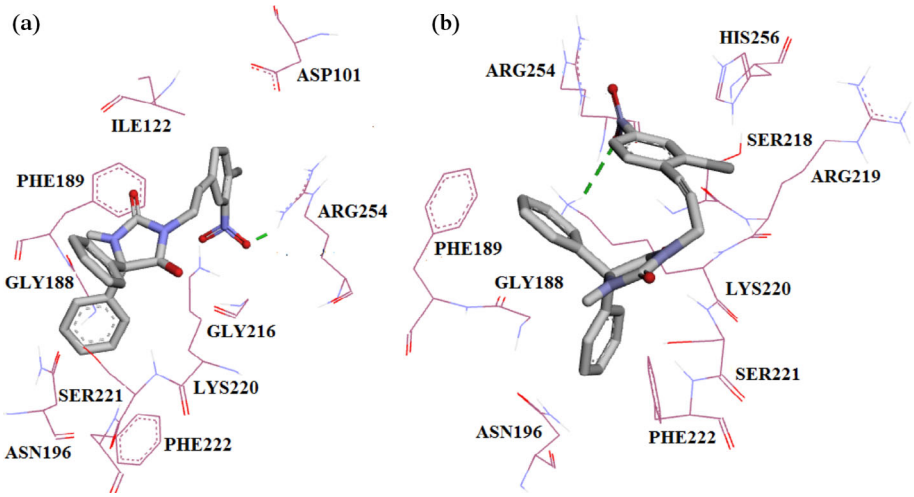

FIGURE 4 Binding mode of compounds **5f** (a) and **5g** (b) with dihydropteroate synthase active site

actions with key residues (LYS220 and ARG254). Whereas, **5d** did not form any cation-π stacking interaction.

Compound **5f** having two groups of chlorine and nitro on *para* and *meta* position, respectively, showed antibacterial activity similar to compounds **5b** and **5d** and free binding energy lower than these two compounds. Compound **5f** has two electron-withdrawing groups with lipophilic and hydrophilic characters while compounds **5d** and **5e** have electron-donating group (methyl and methoxy). Moreover, compound **5f** did not show any cation-π and π-π stacking interactions with active site amino acids.

Compound **5g** revealed poor antibacterial activity and free binding energy than compound **5f**. Both compounds have similar groups on phenyl ring (Cl and NO_2) but positions of two groups on phenyl ring are different. In compound **5f**, chlorine and nitro groups are on *para* and *meta* positions, respectively, while in compound **5g**, chlorine and nitro groups are on *ortho* and *para* positions of phenyl ring (Figure 4). Thus, the position of groups on the phenyl ring might be important for activity and score docking. In addition, compound **5g** formed π-π stacking interaction with PHE189 and two hydrogen bonds with ARG254 (bond length: 1.73 Å) and LYS220 (bond length: 2.79 Å) residues. It seems that π-π stacking interaction and extra hydrogen bond has a negative effect.

Compounds **5a** and **5c** having a strong electron-withdrawing group with the hydrophilic character on phenyl ring displayed the weakest antibacterial activity and free binding energy among compounds. There is NO_2 group on *meta* and *para* positions on phenyl ring in **5a** and **5c**, respectively (Figure 5). Compound **5a** formed a cation-π stacking interaction with ARG254 residue and two hydrogen bonds with LYS220 (bond length: 2.12 Å) and ARG254 (bond length: 1.83 Å) residues. Compound **5c** formed two hydrogen bonds with ARG254 (bond length: 1.61 Å) and SER221 (bond length: 2.01 Å) residues and two π-π stacking interactions with HIS256 and PHE189 amino acids.

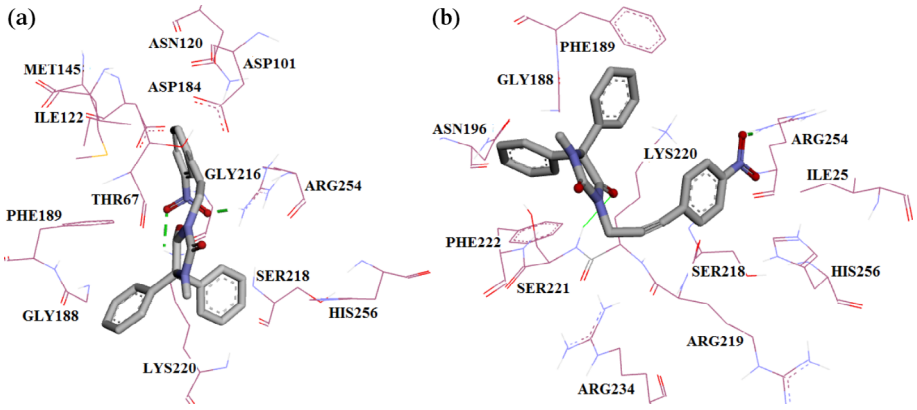

FIGURE 5 Binding mode of compounds **5a** (a) and **5c** (b) with dihydropteroate synthase active site

In summary, the formation of π-π stacking interaction and extra hydrogen bond decreases antibacterial activity and free binding energy of compounds (e.g., compounds **5c** and **5g**). While the presence of cation-π stacking interaction has a positive effect (e.g., compounds **5b** and **5e**). All compounds formed a hydrogen bond with ARG254 residue. According to in vitro and in silico results, the presence of electron-withdrawing and hydrophilic group decreases antibacterial activity and free binding energy whereas, electron-donating and the lipophilic group has a positive effect. In addition, the position of groups on the phenyl ring is important for activity and score docking. Finally, compounds **5b**, **5d**, and **5e** revealed more electrostatic interaction than other compounds (Table 5). Then, the existence of electrostatic interaction also has a positive effect on activity and score docking. Furthermore, the achieved in silico results mention that LYS220 and ARG254 residue were significant residues in keeping the energetic conformations of the screened compounds into DHP enzyme.

3 | EXPERIMENTAL

3.1 | Palladium(II) chloride and propargyl bromide were purchased from Sigma-Aldrich

Triphenylphosphine, *N*,*N*-dimethylformamide, triethylamine, thin-layer chromatography (TLC) plates, silica gel (particle size, 100–200 mesh), and all the solvents used for the reactions were purchased from Merck. NMR spectra were recorded on a Bruker 300 MHz 1H NMR, 75 MHz ^{13}C spectrometer. ^{1}H NMR spectra were reported relative to residual $CHCl_3$ (δ 7.26). ^{13}C NMR spectra were reported relative to $CDCl_3$ (δ 77.16). IR spectra were recorded on a Shimadzu IR-435 grating spectrophotometer. Mass spectra were recorded on a 5975C spectrometer manufactured by Agilent Technologies Company. Elemental analyses were performed on an Eager 300 for EA1112 microanalyzer.

3.2 | Synthesis of 5,5-diphenyl-3-(prop-2-yn-1-yl)imidazolidine-2,4-dione (3)

3-Bromoprop-1-yne (**4**) (1.2 mmol) was added slowly to a stirring mixture of 5,5-diphenylimidazolidine-2,4-dione (**1**) (1 mmol) and K_2CO_3 (1.2 mmol) in dry DMF (3 ml) at room temperature, and stirring was continued till the disappearance of compound **1** (monitored by TLC). The solvent was evaporated to dryness, the residue was washed with H_2O, and dried.[28] White powder solid (95% yield): mp, 194–195°C.

3.3 | General procedure for synthesis of 3-(3-(aryl)prop-2-yn-1-yl)-5,5-diphenylimidazolidine-2,4-dione (5a–g)

To a mixture of aryl iodides **4** (1.0 mmol) and Et_3N (4 mmol) in CH_3CN (4 ml) was added 5,5-diphenyl-3-(prop-2-yn-1-yl)imidazolidine-2,4-dione **3** (1.2 mmol) and stirred at room temperature for 10 hr. Upon completion of the reaction (TLC), the solvent was evaporated and solid obtained was washed with H_2O and subsequently dried. The crude product was purified by column chromatography (silica gel 100) using *n*-hexane/ethyl acetate (97:3) as the eluent.

3.3.1 | 3-(3-(3-Nitrophenyl)prop-2-yn-1-yl)-5,5-diphenylimidazolidine-2,4-dione (5a)

White powder solid (90% yield): mp, 105–107°C; IR (KBr): 3,297 (NH), 3,082, 2,975, 2,926, 1,772 (C═O), 1,714 (C═O), 1,530 (NO_2), 1,446, 1,414, 1,348 (NO_2), 1,257,

1,200, 1,120, 870, 767 cm^{-1}; ^{1}H-NMR (300 MHz, $CDCl_3$): δ 4.62 (s, 2H, CH_2), 7.39–7.48 (m, 11H, PhH, and ArH), 7.52 (d, J = 8.1 Hz, 1H, ArH), 7.71 (d, J = 7.8 Hz, 1H, ArH), 8.18–8.22 (m, 1H, ArH), 8.26 (s, 1H, NH) ppm; ^{13}C-NMR (75 MHz, $CDCl_3$): δ 28.9, 70.5, 81.0, 85.0, 123.4, 124.0, 126.8, 126.9, 128.8, 128.9, 129.3, 137.6, 138.8, 148.0, 155.5, 172.3 ppm; m/z $[M]^+$ 411. Anal. calcd. for $C_{24}H_{17}N_3O_4$: C, 70.07; H, 4.17; N, 10.21; found: C, 70.12; H, 4.19; N, 10.25%.

3.3.2 | 5,5-Diphenyl-3-(3-phenylprop-2-yn-1-yl)imidazolidine-2,4-dione (5b)

Yellow powder solid (87% yield): mp, 102–103°C; IR (KBr): 3,310 (NH), 3,070, 2,925, 2,847, 1,771 (C═O), 1,715 (C═O), 1,559, 1,532, 1,490, 1,443, 1,350, 1,252, 1,209, 1,174, 940, 707 cm^{-1}; ^{1}H-NMR (300 MHz, DMSO-d_6): δ 4.54 (s, 2H, CH_2), 7.36–7.47 (m, 15H, ArH, and ArH), 9.85 (s, 1H, NH) ppm; ^{13}C-NMR (75 MHz, DMSO-d_6): δ 28.9, 69.8, 82.6, 84.3, 122.0, 127.1, 128.8, 129.1, 129.2, 129.4, 131.9, 139.8, 154.7, 172.9 ppm; m/z $[M]^+$ 366. Anal. calcd. for $C_{24}H_{18}N_2O_2$: C, 78.67; H, 4.95; N, 7.65; found: C, 78.64; H, 4.97; N, 7.60%.

3.3.3 | 3-(3-(4-Nitrophenyl)prop-2-yn-1-yl)-5,5-diphenylimidazolidine-2,4-dione (5c)

Yellow powder solid (96% yield): mp, 110–111°C; IR (KBr): 3,300 (NH), 3,050, 2,987, 1,769 (C═O), 1,718 (C═O), 1,597, 1,520 (NO_2), 1,433, 1,345 (NO_2), 1,107, 1,043, 985, 851, 774 cm^{-1}; ^{1}H-NMR (300 MHz, DMSO-d_6): δ 4.31 (s, 2H, CH_2), 7.37–7.47 (m, 10H, ArH), 7.65 (d, J = 9 Hz, 2H, ArH), 8.18 (d, J = 8.7 Hz, 2H, ArH), 9.79 (s, 1H, NH) ppm; ^{13}C-NMR (75 MHz, DMSO-d_6): δ 28.6, 71.4, 83.5, 86.1, 128.8, 131.2, 131.4, 134.8, 135.0, 141.2, 144.5, 147.3, 156.7, 173.1 ppm; m/z $[M]^+$ 411. Anal. calcd. for $C_{24}H_{17}N_3O_4$: C, 70.07; H, 4.17; N, 10.21; found: C, 70.01; H, 4.13; N, 10.20%.

3.3.4 | 3-(3-(4-Methoxyphenyl)prop-2-yn-1-yl)-5,5-diphenylimidazolidine-2,4-dione (5d)

White powder solid (82% yield): mp, 98–100°C; IR (KBr): 3,335 (NH), 3,020, 2,965, 1,764 (C═O), 1,720 (C═O), 1,598, 1,530, 1,458, 1,348, 1,230, 1,100, 1,051, 980, 840, 765 cm^{-1}; ^{1}H-NMR (300 MHz, DMSO-d_6): δ 3.90 (s, 3H, OCH_3), 4.54 (s, 2H, CH_2), 7.19 (d, J = 8.7 Hz, 2H, ArH), 7.35–7.38 (m, 10H, PhH), 7.99 (d, J = 9 Hz, 2H, ArH), 9.77 (s, 1H, NH) ppm; ^{13}C-NMR (75 MHz, DMSO-d_6): δ 34.2, 58.8, 69.8, 82.7, 85.9, 125.2, 127.2, 128.7, 129.0, 136.1, 140.0, 148.5, 155.3, 157.6, 173.3 ppm; m/z $[M]^+$ 396. Anal. calcd. for $C_{25}H_{20}N_2O_3$: C, 75.74; H, 5.09; N, 7.07; found: C, 75.82; H, 5.10; N, 7.03%.

3.3.5 | 5,5-Diphenyl-3-(3-(p-tolyl)prop-2-yn-1-yl)imidazolidine-2,4-dione (5e)

Yellow powder solid (80% yield): mp, 106–107°C; IR (KBr): 3,312 (NH), 3,082, 2,995, 1,769 (C═O), 1,712 (C═O), 1,600, 1,550, 1,488, 1,446, 1,331, 1,254, 1,209, 1,120, 1,046, 940 cm^{-1}; ^{1}H-NMR (300 MHz, DMSO-d_6): δ 2.30 (s, 3H, CH_3), 4.31 (s, 2H, CH_2), 7.37–7.55 (m, 14H, PhH, and ArH), 9.79 (s, 1H, NH) ppm; ^{13}C-NMR (75 MHz, DMSO-d_6): δ 22.8, 33.7, 69.8, 82.8, 86.1, 128.9, 131.2, 132.1, 134.8, 135.0, 137.5, 144.3, 149.0, 156.7, 173.6 ppm; m/z $[M]^+$ 380. Anal. calcd. for $C_{25}H_{20}N_2O_2$: C, 78.93; H, 5.30; N, 7.36; found: C, 78.90; H, 5.33; N, 7.40%.

3.3.6 | 3-(3-(4-Chloro-3-nitrophenyl)prop-2-yn-1-yl)-5,5-diphenylimidazolidine-2,4-dione (5f)

White powder solid (83% yield): mp, 115–118°C; IR (KBr): 3,300 (NH), 3,075, 2,928, 1,772 (C═O), 1,712 (C═O), 1,589, 1,580, 1,500 (NO_2), 1,461, 1,345 (NO_2), 12,365, 1,208, 1,139, 1,112, 873, 779 cm^{-1}; ^{1}H-NMR (300 MHz, DMSO-d_6): δ 4.84 (s, 2H, CH_2), 7.35–7.45 (m, 10H, PhH), 8.03 (d, J = 8.7 Hz, 1H, ArH), 8.30 (dd, J = 8.8, 2.5 Hz, 1H, ArH), 8.72 (d, J = 2.4 Hz, 1H, ArH), 9.75 (s, 1H, NH) ppm; ^{13}C-NMR (75 MHz, DMSO-d_6): δ 33.8, 69.9, 84.1, 87.5, 122.5, 125.0, 125.2, 127.2, 128.7, 129.0, 136.9, 139.4, 144.0, 148.5, 155.9, 173.3 ppm; m/z $[M]^+$ 445. Anal. calcd. for $C_{24}H_{16}ClN_3O_4$: C, 64.65; H, 3.62; N, 9.42; found: C, 64.69; H, 3.60; N, 9.45%.

3.3.7 | 3-(3-(2-Chloro-4-nitrophenyl)prop-2-yn-1-yl)-5,5-diphenylimidazolidine-2,4-dione (5g)

Yellow powder solid (81% yield): mp, 120–122°C; IR (KBr): 3,298 (NH), 3,065, 2,980, 1,775 (C═O), 1,712 (C═O), 1,590, 1,530 (NO_2), 1,491, 1,447, 1,350, 1,235, 1,134, 1,048, 820, 776 cm^{-1}; ^{1}H-NMR (300 MHz, DMSO-d_6): δ 4.88 (s, 2H, CH_2), 7.37–7.43 (m, 10H, PH), 8.03 (d, J = 9 Hz, 1H, ArH), 8.41 (dd, J = 8.7, 2.4 Hz, 1H, ArH), 8.63 (d, J = 1.8 Hz, 1H, ArH), 9.72 (s, 1H, NH) ppm; ^{13}C-NMR (75 MHz, DMSO-d_6): δ 33.7, 69.6, 84.8, 88.2, 124.1, 126.3, 126.8, 127.8, 129.7, 129.8, 131.3, 139.5, 143.3, 148.8,

153.9, 173.8 ppm; *m/z* $[M]^+$ 445. Anal. calcd. for $C_{24}H_{16}ClN_3O_4$: C, 64.65; H, 3.62; N, 9.42; found: C, 64.72; H, 3.65; N, 9.40%.

3.4 | Molecular docking study

Computer-simulated docking studies were accomplished by the AutoDock 4.2.[29] Lamarckian Genetic Algorithm of the AutoDock 4.2 program was used as the search algorithm.[30] The Graphical User Interface program AutoDock Tools 1.5.6 (ADT) was used to prepare, run, and analyze the docking simulations. Molecular docking of compounds was performed with crystal structure DHP (PDB ID: 3TYE) by the Auto-Dock Tool 1.5.6. All two-dimensional (2D) structures of the compounds were built using the ChemDraw program (ChemDraw Ultra 10.0, Cambridge soft.), and then moved into the Hyperchem 8.0 software (HyperChem, Release 8.0 for Windows, Molecular Modeling System: HyperCube, 2007). Molecules were subjected to energy minimization with MM+ force field and then PM3 semi-empirical technique. Then the partial charges of atoms were calculated by the Gasteiger–Marsili procedure implemented in the AutoDock Tools package. The non-polar hydrogens of compounds were merged. The crystal structures of protein were taken from the Protein Data Bank (www.rcsb.org). All bound water and ligands were eliminated from the protein, and polar hydrogen atom was added to the protein as it was required for the electrostatic interactions, and then non-polar hydrogen atoms were merged. In all dockings, a grid map with 60 grid points in the X, Y, and Z directions was built. Among the three different search algorithms offered by AutoDock 4.2, the Lamarckian genetic algorithm approach was applied. For all docking procedures, 150 independent runs with the step sizes of 0.2 Å for translations and 5° for orientations and torsions were considered. For the Lamarckian GA method, a maximum number of 25×10^5 energy evaluations; 27,000 maximum generations; a gene mutation rate of 0.02; and a cross-over rate of 0.8 were used. At the end of the docking, the structures were ranked by energy. Ligand-receptor interactions were all visualized based on docking results using Discovery Studio Visualizer 4.0 and Ligplus 2012.

4 | CONCLUSIONS

We have successfully synthesized a variety of biologically active novel 3-(3-(aryl)prop-2-yn-1-yl)-5,5-diphenyl imidazolidine-2,4-diones from 5,5-diphenyl-3-(prop-2-yn-1-yl)imidazolidine-2,4-dione and aryl iodides via Sonogashira coupling in high to excellent yields. All of the synthesized compounds were examined against the tow bacterial strains *Micrococcus luteus* and *Pseudomonas aeruginosa*. According to the results obtained, compounds **5b**, **5d**, **5e**, and **5f** have the most inhibitory activity against *M. luteus* and **5d** and **5f** have better inhibitory activity than the others against *P. aeruginosa*. The molecular docking study carried out to predict the conformation of the tested compounds recommended that these compounds could bind noticeably to key the residues at the active site of DHP.

ACKNOWLEDGMENTS

The authors wish to express their thanks to the Research Council of Shahrood University of Technology for the financial support of this research work.

ORCID

Ali Keivanloo https://orcid.org/0000-0003-1430-7399

REFERENCES

[1] K. Sonogashira, Y. Tohda, N. Hagihara, *Tetrahedron Lett.* **1975**, *16*, 4467.
[2] T. Hundertmark, A. F. Littke, S. L. Buchwald, G. C. Fu, *Org. Lett.* **2000**, *2*, 1729.
[3] I. Paterson, R. D. M. Davies, R. Marquez, *Angew. Chem.* **2001**, *113*, 623.
[4] M. Kort, V. Correa, A. R. P. M. Valentijn, G. A. Marel, B. V. L. Potter, C. W. Taylor, J. H. Boom, *J. Med. Chem.* **2000**, *43*, 3295.
[5] O. Mongin, L. Porres, L. Moreaux, J. Mertz, M. Blanchard-Desce, *Org. Lett.* **2002**, *4*, 719.
[6] O. Mongin, C. Papamicael, N. Hoyler, A. Gossauer, *J. Org. Chem.* **1998**, *63*, 5568.
[7] A. Baeyer, *Justus Liebigs Ann. Chem.* **1861**, *119*, 126.
[8] (a) D. M. Whitehead, F. L. Strat, S. J. Conway, *Org. Biomol. Chem.* **2008**, *6*, 988. (b) D. Sergent, Q. Wang, A. N. Sasaki, J. Ouazzani, *Bioorg. Med. Chem. Lett.* **2008**, *18*, 4332.
[9] (a) S. M. Dumbris, D. J. Díaz, L. McElwee-White, *J. Org. Chem.* **2009**, *74*, 8862. (b) S. Werner, D. M. Turner, P. G. Chambers, K. M. Brummond, *Tetrahedron* **2008**, *64*, 6997.
[10] D. Zhang, D. Ye, E. Feng, J. Wang, J. Shi, H. Jiang, H. Liu, *J. Org. Chem.* **2010**, *75*, 3552.
[11] C. A. Kumar, S. N. Swamy, K. Sugahara, K. S. Rangappa, *Bioorg. Med. Chem.* **2009**, *17*, 4928.
[12] P. T. Todorov, E. D. Naydenova, *C. R. Chim.* **2010**, *13*, 1424.
[13] A. Mandal, R. S. G. Krishnan, S. Thennarasu, S. Panigrahi, A. B. Mandal, *Colloids Surf. B Biointerfaces* **2010**, *79*, 136.
[14] A. Volonterio, A. C. de Ramirez, M. Zanda, *J. Org. Chem.* **2005**, *70*, 2161.
[15] Y. Brouillette, V. Lisowski, J. Guillon, S. Massip, J. Martinez, *Tetrahedron* **2007**, *63*, 7538.
[16] A. Alizadeh, E. Sheikhi, *Tetrahedron Lett.* **2007**, *48*, 4887.
[17] Y. D. Gong, H. Y. Sohn, M. J. Kurth, *J. Org. Chem.* **1998**, *63*, 4854.
[18] N. Trišović, T. Timić, J. Divljaković, J. Rogan, D. Poleti, M. M. Savić, G. Uščumlić, *Monatsh. Chem.* **2012**, *143*, 1451.
[19] J. Marton, J. Enisz, S. Hosztafi, T. Timar, *J. Agric. Food Chem.* **1993**, *41*, 148.

[20] V. M. Patel, K. R. Desai, *Indian J. Chem.* **2005**, *44B*, 1084.
[21] (a) A. Keivanloo, S. Abbaspour, M. Bakherad, B. Notash, *Chem. Select.* **2019**, *4*, 1366. (b) T. Besharati-Seidani, A. Keivanloo, B. Kaboudin, A. Yoshida, T. Yokomatsu, *Tetrahedron* **2017**, *74*, 2350.
[22] A. Keivanloo, S. S. Kazemi, H. Nasr-Isfahani, A. Bamoniri, *Mol. Divers.* **2017**, *21*, 29.
[23] C. A. Lopez, G. G. Trigo, *Adv. Heterocycl. Chem.* **1985**, *38*, 177.
[24] P. Kellam, W. S. Dallas, S. P. Ballantine, C. J. Delves, *FEMS Microbiol. Lett.* **1995**, *134*, 165.
[25] H. G. Vinnicombe, J. P. Derrick, *Biochem. Biophys. Res. Commun.* **1999**, *258*, 752.
[26] N. Borazjani, S. Sepehri, M. Behzadi, A. Jarrahpour, J. A. Rad, M. Sasanipour, M. Mohkam, Y. Ghasemi, A. R. Akbarizadeh, C. Digiorgio, J. M. Brunel, *Eur. J. Med. Chem.* **2019**, *179*, 389.
[27] M. K. Yun, Y. Wu, Z. Li, Y. Zhao, M. B. Waddell, A. M. Ferreira, R. E. Lee, D. Bashford, S. W. White, *Science* **2012**, *335*, 1110.
[28] S. Abbaspour, A. Keivanloo, M. Bakherad, S. Sepehri, *Chem. Biodivers.* **2019**, *16*, e1800410.
[29] S. Sepehri, L. Saghaie, A. Fassihi, *Mol. Inform.* **2017**, *36*, 1600060.
[30] G. M. Morris, D. S. Goodsell, R. S. Halliday, R. Huey, W. E. Hart, R. K. Belew, A. J. Olson, *J. Comput. Chem.* **1998**, *19*, 1639.

SUPPORTING INFORMATION

Additional supporting information may be found online in the Supporting Information section at the end of this article.

How to cite this article: Keivanloo A, Lashkari S, Sepehri S, Bakherad M, Abbaspour S. Synthesis of hydantoin alkynes through palladium-catalyzed reaction, antibacterial evaluation, and molecular docking studies. *J Chin Chem Soc*. 2021;1–11. https://doi.org/10.1002/jccs.202000475